# Simulation of HTS Josephson mixers

Colin Pegrum, Ting Zhang, Jia Du and Yingjie Jay Guo

***Abstract*—CSIRO has developed superconducting Microwave Monolithic Integrated Circuit (MMIC) mixers using step-edge Josephson junctions and on-chip filters, made from YBaCuO on MgO substrates. Integration into a MMIC results in a compact and efficiently-coupled structure. These have been shown to have outstanding conversion efficiency, dynamic range and linearity.**

**We report here a range of simulations of this type of mixer. We have mainly used Josephson simulators and analyse the data in both the time and frequency domains. More recently we also use microwave simulators incorporating a novel Verilog-A Josephson junction model that we have developed. We have looked at the interactions of junction bias current, local oscillator power and RF input power with conversion efficiency, dynamic range and linearity. Good agreement is found overall with measurements.**

***Index Terms*—MMIC, Superconducting microwave devices, Josephson mixers, heterodyning.**

## I. Introduction

CSIRO has recently demonstrated a range of single-junction externally-pumped mixers, which use an HTS step-edge junction [1], [2], a radio-frequency (RF) input bandpass filter (BPF), a low-pass filter (LPF) at the output intermediate frequency (IF) and a transmission-line resonator for the local oscillator (LO) input (which stops RF leakage back into the LO port). All components are integrated as a Monolithic Microwave Integrated Circuit (MMIC) on a single MgO substrate. This results in a compact and efficiently-coupled structure. Details about the CSIRO HTS step-edge junction technology can be found in [1] and [2]. The filter design and performance is described in [3]–[5].

First-generation devices operated typically at 7 to 12 GHz [6]–[8] and recently a 30 to 33 GHz Ka device been reported [9]. Fig. 1 shows a packaged MMIC with a $10-12$ GHz BPF, a 4 GHz cut-off LPF and an 8 GHz LO filter [6]. Fig. 2 shows its interconnections. The simulation results reported here relate to this device.

## II. Background to HTS Josephson mixers

Suzuki *et al*. [10] and Yoshikawa *et al*. [11] demonstrated an HTS MMIC Josephson mixer which is similar to our design, with RF, LO and IF filters; their later design [12] used on-chip patch antennas to collect the RF and LO signals from a horn antenna. They did not model the behaviour of either device. The mixer reported by Yamaguchi *et al*. [13] used the resitively-shunted junction model (RSJ) for modelling, with junction capacitance included. More recently Malnou *et al*. [14], [15] have demonstrated and modelled HTS Josephson mixers with LO frequencies between 20 and 140 GHz. These have an on-chip wide-band spiral antenna, to which the LO and RF signal are fed via a parabolic mirror and hemispherical lens; their IF bandpass filter is not on-chip. The analysis in [15] uses the RSJ model with capacitance neglected and the three-port technique developed by Taur [16].

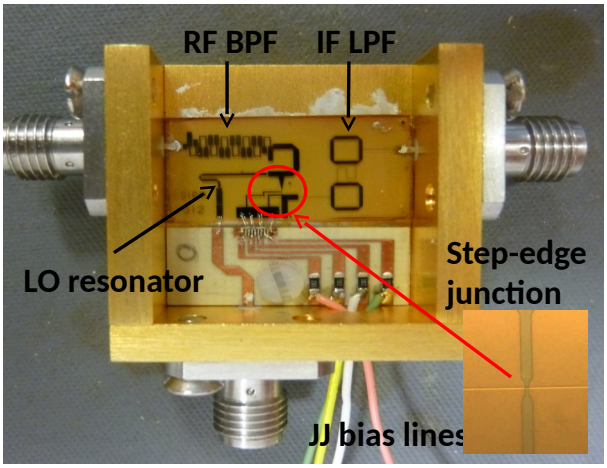


Fig. 1. Photo of a packaged HTS MMIC, with $10-12$ GHz input and 8 GHz LO, taken from [6]. The MgO substrate is $10\,\mathrm{mm} \times 20\,\mathrm{mm}$. The inset shows the $2\,\mu$m wide step-edge junction.

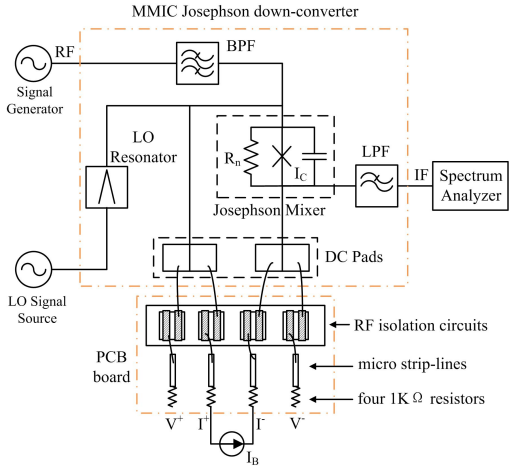


Fig. 2. Schematic of the MMIC in Fig. 1 and the measurement set-up (taken from [6] Fig. 2).

Manuscript received 8 September 2015. Colin Pegrum is with the Department of Physics, University of Strathclyde, Glasgow G4 0NG, UK (e-mail: colin.pegrum@strath.ac.uk).

Ting Zhang is with CSIRO, Lindfield, NSW 2070, Australia (e-mail: ting.zhang@csiro.au).

Jia Du is with CSIRO, Lindfield, NSW 2070, Australia (e-mail: jia.du@csiro.au).

Yingjie Jay Guo is with the University of Technology, Sydney, Australia (e-mail: jay.guo@uts.edu.au).

Our MMIC HTS mixers differ from most of these: they have all filters on chip with 50 ohm connections, and in general the junction capacitance is significant and cannot be neglected — at low temperatures some of the junctions are hysteretic [2]. So our long-term aim is to develop a procedure that can accurately simulate such MMIC mixers.

## III. Modelling approaches

We have recently adopted two different strategies to model our MMIC mixer. The first uses Agilent's Advanced Design System (ADS) [17], a high-performance microwave design and simulation package. We adapted a Josephson junction Verilog-A model from [18] and imported this into ADS. We believe this combination is potentially the best way to model a Josepshon MMIC, as it can simulate accurately the various microwave filters based on their thin-film layout and substrate properties. We have reported preliminary results elsewhere recently [19] which agree well with experimental measurements. But this complex package is not widely available to the superconductivity community (or to non microwave engineers) and there are still some issues for simulating Josephson junction using it, which we are investigating currently. So we have also used the well-tried and freely-available Josephson simulator JSIM [20], [21]. This paper reports work using the JSIM approach with various custom post-processing routines.

JSIM has only a simple transmission line model that cannot represent the complex microstrip filters used in the MMIC. Initially we designed instead 50 Ω band-pass and low-pass filters using discrete inductors, capacitors and resistors. But there are serious issues with this approach: the out-of-band impedances of these filters are very different to those of the real microstrip filters, so the broadband behaviour will not be representative, and the large number of components for high-order filters causes JSIM to run unacceptably slowly. So instead we simplified the model to the minimum possible, as in Fig. 3. This uses AC current sources for the RF and LO inputs. These have infinite impedance, so they provide perfect mutual isolation. We expect this simplified model to show the maximum conversion efficiency possible: it has no filter losses, and there are no mismatches to take into account between the filters and the low-resistance junction.

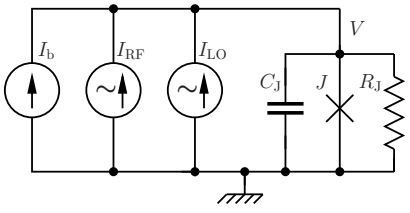


Fig. 3. Our simplified JSIM mixer model. The junction has a DC current source for bias $I_b$. AC current sources $I_{RF}$ and $I_{LO}$ provide RF and LO inputs.

For all simulations reported here, the critical current $I_c = 774\,\mu$A, the junction resistance $R_J = 2.5\,\Omega$, its capacitance $C_J = 18$ fF [22], and the simulation temperature $T = 40$ K in most cases. The RF, LO and IF frequencies $f_{RF}$, $f_{LO}$ and $f_{IF}$ are 10.4, 8 and 2.4 GHz respectively. All these parameters match those of the experimental device [6], so we can compare simulation and experiment. In addition, we have modelled mixers with quite different junction characteristics, e.g. $I_c = 100\,\mu$A, $R_J = 20\,\Omega$, which match the experimental results in [7]. Those results (none are shown here) are qualitatively the same. Note that the latter junction is hysteretic with no RF or LO drive, but with LO turned on, the hysteresis is suppressed.

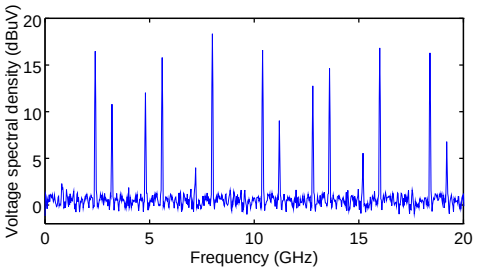


Fig. 4. A typical spectrum, for $f_{RF} = 10.4$ GHz and $f_{LO} = 8$ GHz. Mixing of harmonics of $f_{RF}$ and $f_{LO}$ generates the extra peaks in addition to $f_{IF} = 2.4$ GHz.

## IV. Outline of the simulation procedure

JSIM time-domain data for the mixer output voltage $V(t)$ was generated by parallel processing on a 4 or 8 core CPU. The power spectral density (PSD) of $V(t)$ was got by an Octave or Matlab post-processing script using the pwelch function, with sampling rates and durations set for adequate frequency and amplitude resolution. A typical mixer PSD at $T = 40$ K is shown in Fig. 4. The script locates spectral peaks around the RF, LO and IF frequencies in the PSD, using the built-in findpeaks function, with an adaptive amplitude threshold detector, and measures their powers $P_{RF}$, $P_{LO}$ and $P_{IF}$ and the conversion efficiency $\eta = P_{IF}/P_{RF}$. The dynamic resistance $R_d = V_{RF}/I_{RF}$ is also estimated from the voltage amplitude $V_{RF}$ of the RF signal from the PSD. The correct normalisation factors are applied for the Hanning window used (for details see e.g. [23]), and the amplitude and power calibration was confirmed by a test circuit with the junction replaced by just a resistor.

## V. Critical current suppression

We looked first at current-voltage ($I$-$V$) characteristics and the dependence of $I_c(I_{LO})$ on the LO amplitude $I_{LO}$, with no RF input, Figs. 5(a) and (b). We found the $I_c$ suppression varies very linearly with LO amplitude:

$$I_c(I_{LO}) = I_c(0) - I_{LO} \tag{1}$$

as shown in Fig. 5(b). This linearity is also seen in our experimental measurements, Figs. 6(a) and (b), for this single-junction mixer [6]. We saw this previously [24]. We find also that $I_c(I_{LO})$ remains fully suppressed for $I_{LO} > I_c(0)$, both in simulation and experiment. This departure from the Bessel-like response expected for a voltage-driven junction is because the junction is current-driven, and also because the Josephson frequency $f_J \approx 900$ GHz $>> f_{LO}$ [25].

From Figs. 5(b) and 6(a) we can relate the experimental LO power to the LO current amplitude in the simulation; e.g. an LO power of -40 dB is equivalent to a LO amplitude of $302\mu$A.

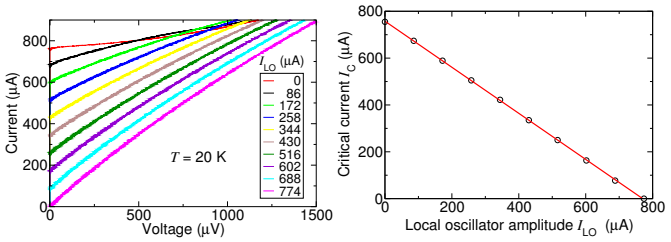


(a) (b)

Fig. 5. Simulation data, (a) a set of $I$-$V$ curves for increasing $I_{\rm LO}$; (b) The critical current suppression is a linear function of $I_{\rm LO}$.

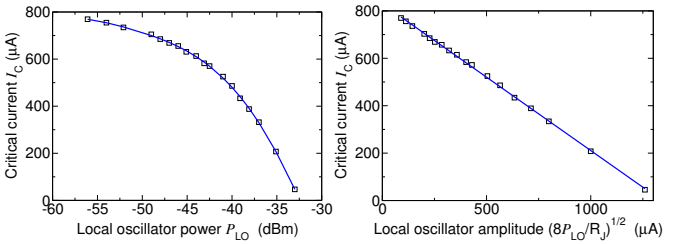


(a) (b)

Fig. 6. Experimental data at $T = 40$ K for the critical current (a) as a function LO power (b) showing its linear dependence on the LO voltage. Data from [6].

## VI. Effects of Noise

Most experimental measurements were done at $T = 40$ K. At this temperature the junction noise-rounding parameter $\Gamma(I_{\rm c}) = (2\pi k_{\rm B}T)/(I_{\rm c}\Phi_0) \approx 2 \times 10^{-3}$ for $I_{\rm c} = 774\,\mu$A, where $k_{\rm B}$ is Boltzmann's constant, and $\Phi_0$ is the flux quantum. So at 40 K thermal noise has little effect on the $I$-$V$ characteristics in the absence of RF or LO input.

In simulations at $T = 0$ K, with LO input at 8 GHz at typical levels, microwave-induced steps can be seen, as in Fig. 7. Their step height $\Delta I_{\rm c} \approx 10\,\mu$A and since $\Gamma(10\,\mu{\rm A}) = 0.17$ at 40 K, these steps are strongly noise-rounded and so we find they are neither visible experimentally at 40 K [6], nor in the simulation in Fig. 5(a) at 20 K. This was also observed in [10].

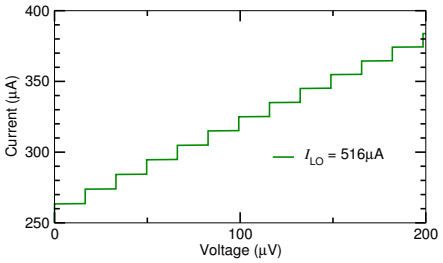


Fig. 7. Part of a simulated $I$-$V$ curve for $I_{\rm c} = 774\,\mu$A at $T = 0$ K, with $f_{\rm LO} = 8$ GHz.

For the simulations described below in Sections VII and VIII we ran some trials at $T = 0, 20$ and 40 K. The results for all were broadly the same and the difference between the 20 K and 40 K results was not significant. Because simulations at 20 K are faster than those at 40 K, for the same signal-to-noise ratio, we ran some at 20 K, but unless shown otherwise, all results here are at $T = 40$ K.

## VII. Dependence on RF and LO Amplitudes

We have looked at the variations of IF output and conversion efficiency with DC bias current $I_{\rm b}$, for a very wide range of LO and RF currents $I_{\rm LO}$ and $I_{\rm RF}$. Some representative results are shown in Figs. 8(a) and (b). It shows that $\eta$ can be as high as -1 dB, which is in line with experimental measurements of -1 dB at 20 K and -3.6 dB at 40 K [6], both of which take into account filter losses and input and output coupling losses in the real MMIC.

A notable feature is a minimum in IF output at a certain value of $I_{\rm b}$; this is also seen in experiments, as in Fig. 8(c). We [6] and others [13] have previously attributed this to a point of inflection in the $I$-$V$ curve. We would expect this to be at the bias current where $R_{\rm d}$ is a maximum. The simulation results in Fig. 9 show that there is indeed a single maximum in $R_{\rm d}$, and like the location of the $V_{\rm IF}$ minimum, it moves to higher $I_{\rm b}$ with increasing $I_{\rm LO}$, however, it appears that the minimum in $V_{\rm IF}$ does not quite coincide with the maximum in our estimate of $R_{\rm d}$. This issue needs further consideration.

## VIII. Linearity

The procedure of Section IV was adapted to study the linearity of the MMIC, by varying $I_{\rm RF}$ for a range of values of $I_{\rm LO}$. Simulated dependencies on $I_{\rm RF}$ of the IF output $V_{\rm IF}$ and the conversion efficiency $\eta$ are shown in Figs. 10(a) and (b), for $I_{\rm b} = 700\,\mu$A.

We see that $\eta$ is constant and the output varies linearly with input, up to the point where $I_{\rm RF} \approx I_{\rm LO}$. Beyond that, there is a linear fall in output, followed by a rapid collapse in the output at high values of $I_{\rm RF}$. Broadly similar features are seen experimentally, as in Fig. 10(c), which shows the behaviour for just one value of $P_{\rm LO}$ [6].

## IX. Conclusions

1. We believe our simulation method is effective, economical and fast, with results which agree well with experiment.
2. In this ideal model, the best conversion efficiency seen was -1 dB for optimum values of $I_{\rm b} \approx 500\,\mu$A and $I_{\rm LO} = 200\,\mu$A. The optimum operating range is with $I_{\rm b}$ well below $I_{\rm c}$, which is always well clear of the point of zero IF output.
3. We find the same dependence of critical current suppression on LO amplitude as we see in experiments. The dependence is linear, and for $I_{\rm LO} > I_{\rm c}(0)$, $I_{\rm c}(I_{\rm LO}) = 0$.
4. Best linearity is obtained with high LO drive, but the best conversion efficiency is with low LO drive.
5. The minimum in IF output at a certain value of $I_{\rm b}$, seen in both experiments and simulations, needs further study; it is not clear why other mixing products do not disappear at this same bias point.

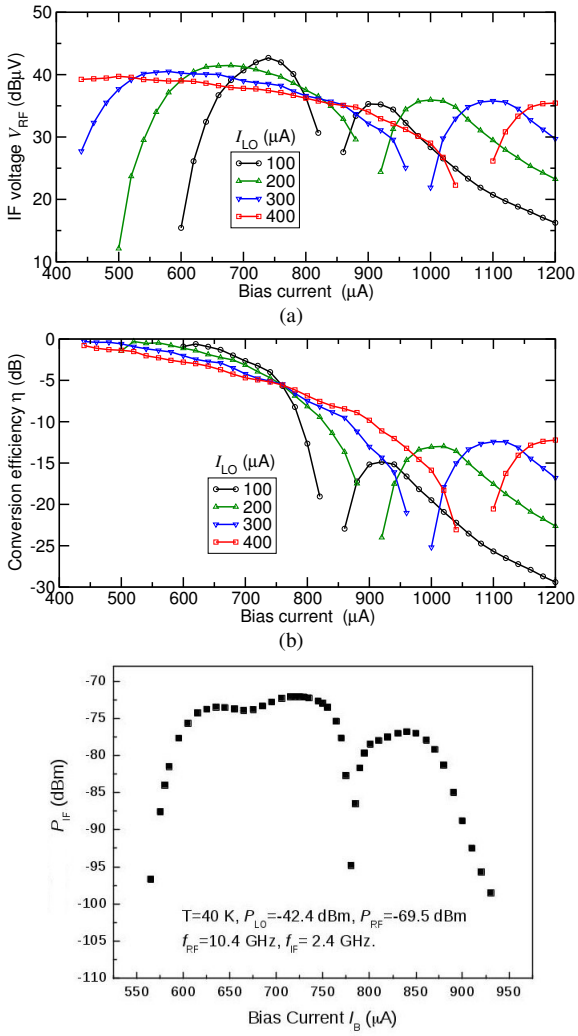


Fig. 8. (a) Simulated IF power and (b) simulated conversion efficiency, as functions of bias current $I_{\rm b}$, at $T = 40\,{\rm K}$, for $I_{\rm RF} = 80\,\mu{\rm A}$. Discontinuities in the data occur where the IF output falls below the noise level and an accurate measure of it cannot be made. (c) Experimental IF power dependence on $I_{\rm b}$, also showing a sharp minimum, taken from [6].

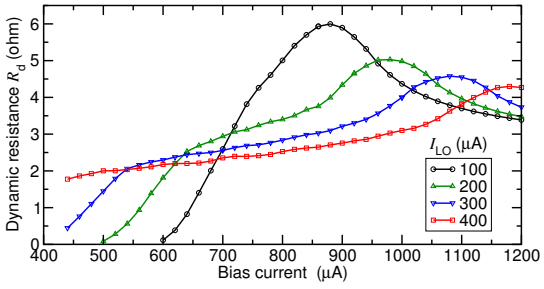


Fig. 9. Estimated dynamic resistance $R_{\rm d}$, from simulation at $T = 40\,{\rm K}$, for $I_{\rm RF} = 80\,\mu{\rm A}$.

## ACKNOWLEDGMENT

We thank our collaborators Dr D. D. Bai and Prof Y. S. He of the Institute of Applied Physics, Chinese Academy of Sciences, for their earlier contributions to the experimental results presented in [6].

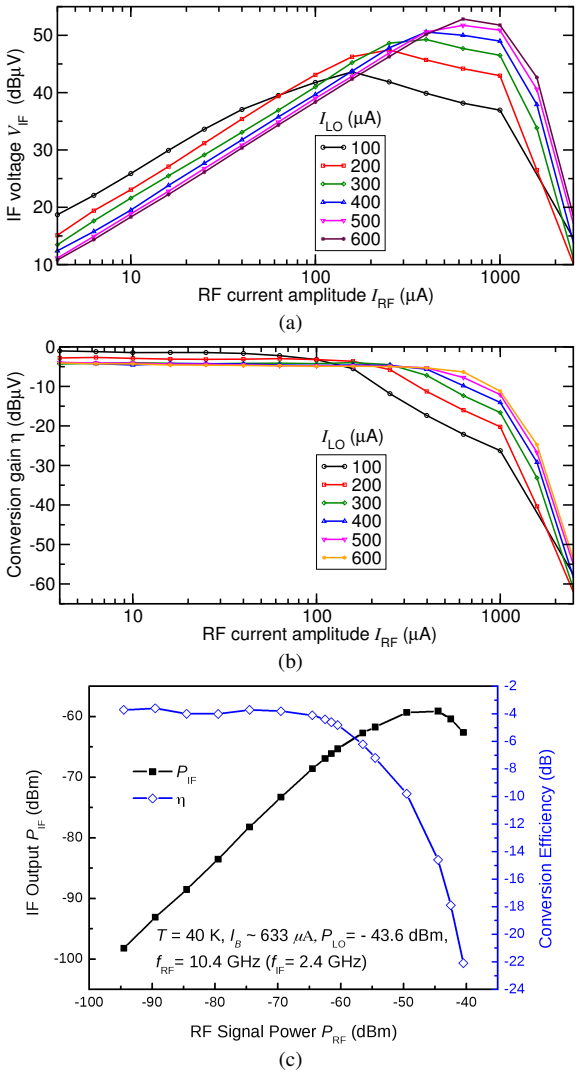


Fig. 10. (a) Simulated IF output voltage amplitude as a function of RF current amplitude, for a range of values of $I_{\rm LO}$, (b) A similar plot for simulated conversion efficiency $\eta$. (c) Experimental data for $P_{\rm IF}$ and $\eta$, as a function of RF power $P_{\rm RF}$, taken from [6].

## REFERENCES

[1] C. Foley, E. Mitchell, S. Lam, B. Sankrithyan, Y. Wilson, D. Tilbrook, and S. Morris, "Fabrication and characterisation of YBCO single grain boundary step edge junctions," *IEEE Trans. Appl. Supercond.*, vol. 9, no. 2, pp. 4281–4284, Jun. 1999.

[2] E. E. Mitchell and C. P. Foley, "YBCO step-edge junctions with high $I_{\rm c}R_{\rm n}$," *Supercond. Sci. Technol.*, vol. 23, no. 6, p. 065007, Jun. 2010.

[3] T. Zhang, J. Du, Y. Guo, and X. W. Sun, "On-chip integration of HTS bandpass and lowpass filters with Josephson mixer," *Electron. Lett.*, vol. 48, no. 12, pp. 729–731, 2012.

[4] T. Zhang, J. Du, Y. J. Guo, and X. Sun, "Design and integration of HTS filters with a Josephson device," *Supercond. Sci. Technol.*, vol. 25, no. 10, p. 105014, 2012.

[5] D. D. Bai, J. Du, T. Zhang, and Y. S. He, "A compact high temperature superconducting bandpass filter for integration with a Josephson mixer," *J. Appl. Phys.*, vol. 114, no. 13, p. 133906, 2013.

[6] J. Du, D. D. Bai, T. Zhang, Y. J. Guo, Y. S. He, and C. M. Pegrum, "Optimised conversion efficiency of a HTS MMIC Josephson down-converter," *Supercond. Sci. Technol.*, vol. 27, no. 10, p. 105002, 2014.

[7] J. Du, T. Zhang, Y. J. Guo, and X. W. Sun, "A high-temperature superconducting monolithic microwave integrated Josephson down-converter with high conversion efficiency," *Appl. Phys. Lett.*, vol. 102, no. 21, p. 212602, 2013.

[8] T. Zhang, J. Du, Y. Guo, and X. Sun, "A $7-8.5$ GHz high performance MMIC HTS Josephson mixer," *IEEE Microw. Wireless Compon. Lett.*, vol. 23, no. 8, pp. 427–429, Aug. 2013.

[9] T. Zhang, J. Du, J. Wang, D. Bai, Y. Guo, and Y. He, "30 GHz HTS receiver front-end based on monolithic Josephson mixer," *IEEE Trans. Appl, Supercond.*, vol. 25, no. 3, p. 1400605, Jun. 2015.

[10] K. Suzuki, S. Yoshikawa, K. Yamaguchi, K. Hayashi, S. Fujino, T. Takenaka, T. Mitsuzuka, Y. Enomoto, K. Imai, F. Suginoshita, and N. Yazawa, "Noise figure of HTS JJ MMIC downconverter at 12 GHz," in *IEEE MTT-S Digest*, June 1993, pp. 1429–1432.

[11] S. Yoshikawa, K. Yamaguchi, T. Takenaka, S. Fujino, T. Mitsuzuka, K. Hayashi, K. Suzuki, and Y. Enomoto, "X-band mixing performance of YBCO step-edge junction," *J. J. Appl. Phys.*, vol. 33, no. 9A, pp. 4880–4886.

[12] K. Suzuki, K. Hayashi, A. Murphy, M. Fujimoto, S. Yoshikawa, K. Yamaguchi, and Y. Enomoto, "Y-Ba-Cu-O mixer antenna array at 23 GHz," in *IEEE MTT-S Digest*, May 1994, pp. 1001–1004.

[13] K. Yamaguchi, A. Kawaji, K. Suzuki, Y. Enomoto, and S. Tanaka, "IF output characteristics of Josephson mixer," *Electron. Comm. Jpn. 2*, vol. 80, no. 3, pp. 69–79, 1997.

[14] M. Malnou, A. Luo, T. Wolf, Y. Wang, C. Feuillet-Palma, C. Ulysse, G. Faini, P. Febvre, M. Sirena, J. Lesueur, and N. Bergeal, "Toward terahertz heterodyne detection with superconducting Josephson junctions," *Appl. Phys. Lett.*, vol. 101, no. 23, p. 233505, 2012.

[15] M. Malnou, C. Feuillet-Palma, C. Ulysse, G. Faini, P. Febvre, M. Sirena, L. Olanier, J. Lesueur, and N. Bergeal, "High-$T_c$ superconducting Josephson mixers for terahertz heterodyne detection," *J. Appl. Phys.*, vol. 116, no. 7, p. 074505, 2014.

[16] Y. Taur, "Josephson-junction mixer analysis using frequency-conversion and noise-correlation matrices," *IEEE Trans. Electron Devices*, vol. 27, no. 10, pp. 1921–1928, 1980.

[17] Advanced Design System (ADS), Keysight Technologies, http://www.keysight.com/en/pc-1297113/advanced-design-system-ads.

[18] Accellera Systems Initiative, http://accellera.org.

[19] T. Zhang, C. Pegrum, J. Du, and Y. J. Guo, "Modeling and simulation of an HTS MMIC Josephson junction mixer," in *Extended abstracts, Int. Supercond. Electron. Conf, (ISEC'15), Nagoya, Japan*, 2015, paper HF-O06.

[20] E. S. Fang and T. Van Duzer, "A Josephson integrated circuit simulator (JSIM) for superconductive electronics application," in *Extended abstracts, Int. Supercond. Electron. Conf. (ISEC'89), Tokyo, Japan*, 1989, pp. 407–410.

[21] J. Satchell, "Stochastic simulation of SFQ logic," *IEEE Trans. Appl. Supercond.*, vol. 2, no. 7, pp. 3315–3318, Jun. 1997.

[22] H. Töpfer, G. Mäder, and H. Uhlmann, "Accurate calculation of capacitances of grain boundary Josephson junctions in high critical temperature superconductors," *J. Appl. Phys.*, vol. 77, no. 9, pp. 4576–4579, May 1995.

[23] H. Schmid, "How to use the FFT and Matlab's pwelch function for signal and noise simulations and measurements," Aug. 2012, http://www.fhnw.ch/technik/ime/publikationen/2012.

[24] J. Du, J. C. Macfarlane, C. M. Pegrum, T. Zhang, Y. Cai, and Y. J. Guo, "A self-pumped high-temperature superconducting Josephson mixer: Modelling and measurement," *J. Appl. Phys.*, vol. 111, no. 5, p. 053910, 2012.

[25] Y. Taur, J. Claassen, and P. Richards, "Josephson junctions as heterodyne detectors," *IEEE Trans. Microw. Theory Techn.*, vol. 22, no. 12, pp. 1005–1009, 1974.